

# LINEAR OPTICS AND COUPLING CORRECTION WITH TURN-BY-TURN BPM DATA\*

Xiaobiao Huang<sup>†</sup>, SLAC, Menlo Park, CA 94025, USA  
 Xi Yang, BNL, Upton, Long Island, NY 11973, USA

## Abstract

We propose a method to measure and correct storage ring linear optics and coupling with turn-by-turn BPM data. The independent component analysis (ICA) is used to obtain the amplitudes and phase advances of the betatron normal modes, which are compared to their counterparts derived from the lattice model. By fitting the model to the data with quadrupole and skew quadrupole variables, the linear optics and coupling of the machine can be obtained. Simulation demonstrates that errors in the lattice and BPM parameters can be recovered with this method. Experiments on the NSLS-II storage ring show that it can find the same optics as the linear optics from closed orbit (LOCO) method.

## INTRODUCTION

The linear optics of a storage ring is often distorted by various error sources such as systematic and random errors of quadrupole magnets, feed-down effect from orbit offsets in sextupole magnets, and perturbations by insertion devices. The machine with distorted optics has large beta beating and phase advance deviation, which would have a negative impact on the nonlinear beam dynamics performance, resulting in reduced dynamic aperture and/or Touschek lifetime. There is also a need to accurately implement the design optics in order to deliver certain beam properties to users or to facilitate beam diagnostics and beam protection systems. Therefore, optics correction is of crucial importance for storage ring operation. The uncorrected machine may also have a large linear coupling, which needs to be corrected in order to reduce the vertical emittance.

The LOCO method [1] is widely used for both linear optics and coupling correction for storage rings. It fits the measured orbit response matrix data to a lattice model, from which one can derive the required quadrupole and skew quadrupole adjustments for optics and coupling correction. This method is very effective if care is taken to avoid the weakly constrained directions of parameter space from having large contributions in the corrections [2]. A main disadvantage of the LOCO method is that it is time consuming to measure the orbit response matrix. Depending on the size of the ring and the ramp rate of the corrector magnets, the time for measuring the orbit response matrix may vary from 10 min to a few hours.

Similar to the orbit response matrix, turn-by-turn (TBT) BPM data taken when beam undergoes coherent betatron oscillation contain valuable information of the linear optics of the machine. Taking TBT BPM data requires only a few

seconds and is nearly non-invasive to the beam. There have been previous proposals and experimental studies on the use of TBT BPM data to measure and correct optics [3–6]. There have also been studies that utilize TBT BPM data to correct linear coupling [7, 8]. These methods typically treat in-plane optics correction and coupling correction separately, despite the fact that TBT BPM data contain optics and coupling error information simultaneously, much the same as the orbit response matrix data.

In this study we propose a method to simultaneously measure and correct linear optics and coupling with TBT BPM data. Similar to LOCO, quadrupole and skew quadrupole variables in the lattice model are varied to fit the measured data, resulting in a calibrated lattice model. The independent component analysis (ICA) method is employed to retrieve the normal mode components for each BPM, which are then compared to model calculations.

In the following we will give a description of the method and present simulation and experimental results.

## DESCRIPTION OF THE METHOD

With linear coupling, the beam motion observed on each plane of a BPM is a combination of two normal modes. The ICA can separate the normal modes simultaneously for all BPMs and obtain the beam motion at each BPM in a form [3]

$$\begin{aligned} x_n &= A \cos \Psi_1(n) - B \sin \Psi_1(n) + c \cos \Psi_2(n) - d \sin \Psi_2(n), \\ y_n &= a \cos \Psi_1(n) - b \sin \Psi_1(n) + C \cos \Psi_2(n) - D \sin \Psi_2(n), \end{aligned} \quad (1)$$

where  $x_n$  and  $y_n$  are observed beam positions for the  $x$  and  $y$  planes at the  $n$ 'th turn, respectively,  $\Psi_{1,2}(n) = 2\pi\nu_{1,2}n + \psi_{1,2}$ , and  $\nu_{1,2}$  and  $\psi_{1,2}$  are the tunes and initial phases of the normal modes. Note that  $\psi_{1,2}$  are equal for all BPMs.

On the other hand, the phase space coordinates  $X = (x, x', y, y')^T$  are related to the normal mode coordinates

$$\Theta = \begin{pmatrix} \sqrt{2J_1} \cos \Phi_1 \\ -\sqrt{2J_1} \sin \Phi_1 \\ \sqrt{2J_2} \cos \Phi_2 \\ -\sqrt{2J_2} \sin \Phi_2 \end{pmatrix} \quad (2)$$

via a transformation  $X = P\Theta$ , where  $J_{1,2}$  and  $\Phi_{1,2}$  are the action and phase variables for the two normal modes, respectively [9]. Explicitly,

$$\begin{aligned} x &= p_{11}\sqrt{2J_1} \cos \Phi_1 + \sqrt{2J_2}(p_{13} \cos \Phi_2 - p_{14} \sin \Phi_2), \\ y &= \sqrt{2J_1}(p_{31} \cos \Phi_1 - p_{32} \sin \Phi_1) + p_{33}\sqrt{2J_2} \cos \Phi_2, \end{aligned} \quad (3)$$

where we have made use of the fact that  $p_{12} = p_{34} = 0$  by definition of  $P$  and  $\Phi_{1,2}$ . The phase variables  $\Phi_{1,2}$  advance

\* Work supported by DOE Contract No. DE-AC02-76SF00515

<sup>†</sup> xiahuang@slac.stanford.edu

from one location to another and increment by  $2\pi\nu_{1,2}$  in one turn, respectively. Therefore, amplitudes and phases of the normal mode components in the  $x$  and  $y$  planes can be calculated with elements of the  $P$  matrix. The amplitudes are related by

$$\begin{aligned}\sqrt{A^2 + B^2} &= 2J_1 p_{11}, & \sqrt{c^2 + d^2} &= 2J_2 \sqrt{p_{13}^2 + p_{14}^2}, \\ \sqrt{C^2 + D^2} &= 2J_2 p_{33}, & \sqrt{a^2 + b^2} &= 2J_1 \sqrt{p_{31}^2 + p_{32}^2}.\end{aligned}\quad (4)$$

Apart from the initial phases that can be subtracted, the phase variables are related by

$$\begin{aligned}\tan^{-1} \frac{B}{A} &= \text{Mod}_{2\pi}(\Phi_1), \\ \tan^{-1} \frac{d}{c} &= \text{Mod}_{2\pi}(\Phi_2 + \tan^{-1} \frac{p_{14}}{p_{13}}), \\ \tan^{-1} \frac{b}{a} &= \text{Mod}_{2\pi}(\Phi_1 + \tan^{-1} \frac{p_{32}}{p_{31}}), \\ \tan^{-1} \frac{D}{C} &= \text{Mod}_{2\pi}(\Phi_2).\end{aligned}\quad (5)$$

The  $P$  matrix can be computed from the one-turn transfer matrix  $T$  with the numerical procedure given in Ref. [9] or alternatively with equation  $P = VU$ , with matrices  $V$  and  $U$  given by analytic formulas in Ref. [10].

The differences between the measured and calculated amplitudes and phases can be put in a least-square problem, with each term normalized by a suitable uncertainty sigma. The constants  $J_{1,2}$  can be found by equating the average measured and model amplitudes for the in-plane normal modes, i.e., the first and third equations in Eq. (4). Horizontal and vertical dispersion functions can also be measured and included in as fitting data. Errors of the horizontal dispersion function are an important measure of the horizontal linear optics. The vertical dispersion is a major contribution of vertical emittance. Therefore, including the dispersion functions in the least-square problem is important. The three types of contribution in the least-square problems, namely, amplitudes, phases and dispersion functions, may be given different weights to emphasize our confidence in the measurements. For example, the phases could be given higher weight than the amplitudes as the latter is affected by the BPM calibration.

In reality BPMs have calibration and roll errors. These parameters can be included in the fitting scheme. The fitting parameters are the quadrupole and skew quadrupole strengths in the lattice model and the BPM gain and roll parameters. It is helpful to use small random values as initial skew quadrupole variables if the initial lattice has no coupling. This removes the ambiguity of the phases of the secondary modes due to zero coefficients  $a, b, c$  and  $d$  in Eq.(5). It is worth noting that correlation of the fitting parameters can cause the fitting solution to have large excursion along the under-constrained directions in the parameter space, in much the same way as it does to LOCO [2]. Therefore the constrained fitting technique should be used for our present problem.

## 5: Beam Dynamics and EM Fields

### D01 - Beam Optics - Lattices, Correction Schemes, Transport

## SIMULATION

We have done simulation with the SPEAR3 and NSLS-II lattice models to verify the optics and coupling correction approach described in the previous section. For the SPEAR3 case, quadrupole and skew quadrupole errors are inserted into selected magnets in the lattice model. TBT data are generated at the BPMs by tracking, with initial offsets of  $\Delta x = 2.0$  mm and  $\Delta y = 1.0$  mm. Gaussian noise of  $\sigma = 0.02$  mm is added to the tracking data for each BPM. Random BPM gain and roll errors are generated and used to artificially distort the data. The ICA method is applied to separate the normal modes. Figure 1 shows the spatial patterns and the FFT spectra of the ICA modes for half of the decoupled normal modes.

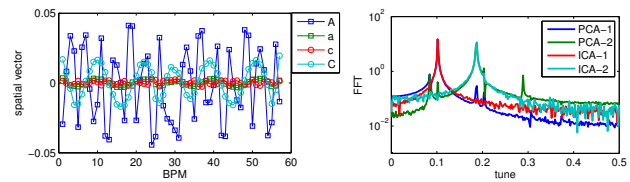


Figure 1: The spatial (left) patterns and FFT spectra (right) of the ICA modes. Right plot also includes the PCA modes.

The spatial patterns are used to calculate the amplitude and phase functions, which are then used in the least-square fitting. The fitting parameters are 72 quadrupole variables, 13 skew quadrupole variables, and horizontal and vertical gains and roll for each of the 57 BPMs. The normalized  $\chi^2$  dropped from 213.6 to 10.2 in two iterations. The fitted lattice parameters agree very well with the target values (Figure 2). The BPM gain and roll errors are also precisely recovered. Both horizontal and vertical beta beats for the initial lattice (relative to the target lattice with artificial errors) are 11% rms. The fitted lattice has a beta beat of less than 0.3%. The local vertical emittance of the fitted lattice is nearly the same as the target.

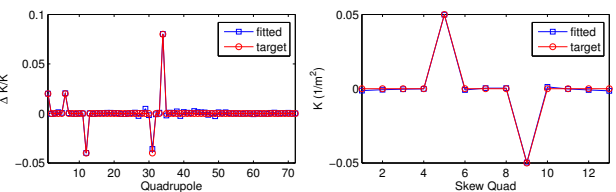


Figure 2: The fitted quadrupole (left) and skew quadrupole (right) variables are compared to the target values for the SPEAR3 simulation.

For simulation with the NSLS-II lattice, a 2% error is added to one quadrupole, while random errors (with rms error of 0.1%) are added to all other quadrupoles. Random skew quadrupole errors and BPM errors are also inserted. BPM noise of 0.02 mm rms is added to the tracking data of all 180 BPMs. The fitting lattice parameters include 150 quadrupole parameters and 30 skew quadrupole parameters, same as used for LOCO [11].

The BPM gain and roll errors are successfully recovered (Figure 3). Because correlation between quadrupole parameters for the NSLS-II lattice is more severe, the fitted

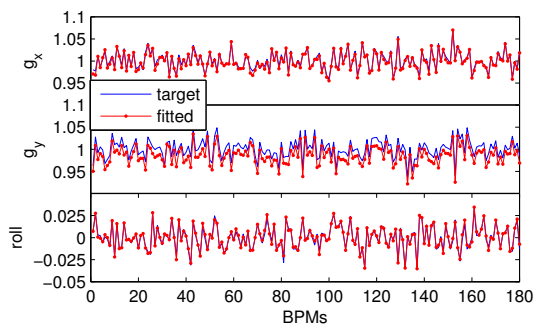


Figure 3: The fitted BPM gains and rolls for the NSLS-II simulation.

quadrupole parameters did not completely recover the errors planted into the model (Figure 4 left). However, the beta beat of the fitted lattice with respect to the target lattice is much reduced from the initial lattice, which indicate the optics of the fitted lattice is more or less equivalent to the target lattice (Figure 5 left plot). The rms beta beats were reduced from 5.3% horizontal and 5.2% vertical to 0.7% horizontal and 0.6% vertical, respectively. The fitted skew quadrupoles reproduced the expected errors accurately (Figure 4 right). The local vertical emittance of the fitted lattice agrees with the target lattice very well, as is shown in Figure 5 right plot.

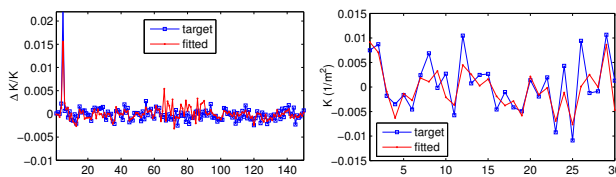


Figure 4: The fitted quadrupole (left) and skew quadrupole (right) variables are compared to the target values for a simulation with the NSLS-II lattice.

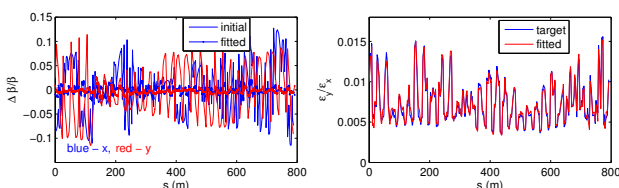


Figure 5: Beta beat (relative to target lattice) of the initial and fitted lattices (left) and comparison of vertical emittances (right) between target and fitted lattices for the NSLS-II simulation.

## EXPERIMENT

We took experimental TBT BPM data for the NSLS-II storage ring when the beam was excited on both transverse planes. The oscillation amplitudes are on average roughly 0.2 mm horizontal and 0.3 mm vertical. The spatial vector and FFT spectra (512 turns are used) of each of the two pairs of ICA normal modes are shown in Figure 6. Because the coupling was corrected before the measurement, the amplitudes of the secondary modes were very small. The ampli-

tudes and phases derived from the spatial vectors are used for fitting the lattice parameters and BPM parameters. Normalized  $\chi^2$  was reduced from 15.6 to 0.20 in four iterations.

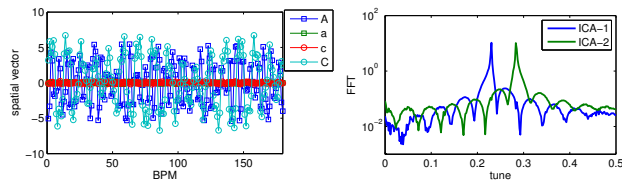


Figure 6: The spatial (left) patterns and FFT spectra (right) of the ICA modes for experimental data from NSLS-II.

LOCO data were taken under the same condition during the same experiment. The LOCO data were fitted for two iterations with normalized  $\chi^2$  reduced from 3865.0 to 6.4. The fitted BPM gains from the ICA and LOCO methods generally agree. The fitted quadrupole parameters and skew quadrupole parameters are compared to the ICA results in Figure 7. There are clear similarity between the fitting results of the two methods. The fitted quadrupole errors from LOCO data are larger than ICA results for some quadrupoles, especially for the QH1 family (parameter 61-90). This could be caused by the degeneracy issue. The beta beats of the fitted lattices for the two methods are very much the same, which are shown in Figure 8. The fitted lattices for both data sets have very small coupling.

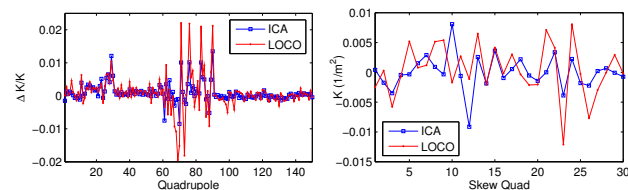


Figure 7: Comparison of fitted quadrupole (left) and skew quadrupole (right) parameters for ICA and LOCO.

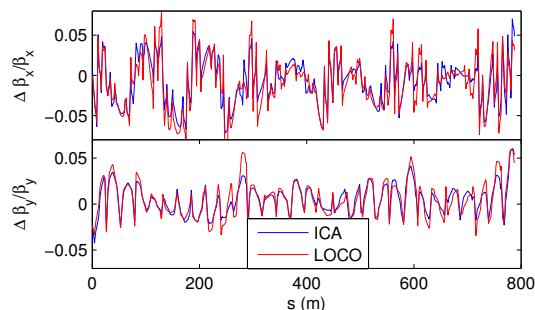


Figure 8: Comparison of beta beats of the fitted lattices for ICA and LOCO for NSLS-II measurements.

## CONCLUSION

We propose a method to measure and correct linear optics and coupling for storage rings using turn-by-turn BPM data. The ICA method and least-square fitting are used to obtain lattice and BPM parameters. We demonstrated this method with both simulation and experimental data.

## REFERENCES

- [1] J. Safranek, Nucl. Instrum. Methods Phys. Res., Sect. A, 388(1-2), 27 (1997).
- [2] X. Huang, et al, ICFA Newsletter 44, 60 (2007).
- [3] X. Huang, et al, Phys. Rev. ST-AB, 8, 064001 (2005).
- [4] X. Huang, et al, Phys. Rev. ST-AB, 13, 114002 (2010).
- [5] R. Tomás, et al, Phys. Rev. ST-AB, 13, 121004 (2010).
- [6] M. Aiba, et al, Phys. Rev. ST-AB, 16, 012802 (2013).
- [7] A. Franchi, et al, Phys. Rev. ST-AB, 14, 034002 (2011).
- [8] M. Takao, et al, IPAC2012, Louisiana, USA (2012).
- [9] Y. Luo, Phys. Rev. ST-AB, 7, 124001 (2004).
- [10] D. Sagan and D. Rubin, Phys. Rev. ST-AB, 2, 074001 (1999).
- [11] X. Yang, et al, IPAC2015, these proceedings. (2015).